

# Damage identification in beams using inverse methods

T. Lauwagie<sup>1</sup>, H. Sol<sup>2</sup>, E. Dascotte<sup>3</sup>

<sup>1</sup> Katholieke Universiteit Leuven, Department of Mechanical Engineering (PMA),  
Celestijnenlaan 300b, 3001 Heverlee, Belgium  
email: [Tom.Lauwagie@mech.kuleuven.ac.be](mailto:Tom.Lauwagie@mech.kuleuven.ac.be)

<sup>2</sup> Vrije Universiteit Brussel (VUB)  
Department Mechanics of Materials and Constructions (MEMC)  
Pleinlaan 2, 1050 Brussels, Belgium  
email: [hugos@vub.ac.be](mailto:hugos@vub.ac.be)

<sup>3</sup> Dynamic Design Solutions (DDS) NV  
Interleuvenlaan 64, 3001 Leuven, Belgium  
email: [Eddy.Dascotte@dds.be](mailto:Eddy.Dascotte@dds.be), [www.femtools.com](http://www.femtools.com)

## Abstract

Beams, made of brittle materials like concrete or cement, show increasing crack development during their service life due to mechanical and environmental loadings. This local damage can be translated into a reduction of the local bending stiffness. Stiffness modifications, while assuming constant mass distribution, can be observed by monitoring the vibrational behavior of the beam. In this paper the modal parameters of an undamaged beam are monitored and compared with the vibration behavior of the beam subjected to controlled damaging. Selected stiffness parameters in the finite element model are adjusted in such a way that the computed modal quantities match the measured quantities. FEMtools has been used to establish a damage distribution in beams associated with increasing stress patterns. State of the art scanning laser modal equipment has been used for this purpose. It has been found that modal updating is indeed a possible tool to reconstruct the damage patterns.

## 1 Introduction

The ability to monitor a structure and detect damage at the earliest possible stage is of utmost importance in the civil, mechanical and aerospace engineering communities. Commonly used damage detection methods are either visual or localized experimental methods such as acoustic or ultrasonic methods, magnetic field methods, radiograph, Eddy current methods and thermal field methods [1]. All of these experimental techniques require that the location of the damage is known a priori and that the portion of the structure being inspected is readily accessible. Subjected to these limitations, these experimental methods can detect damage on or near the surface of the structure. The need for additional global damage detection methods that can be applied to complex structures has led to the development and continued research of methods that examine changes in the vibration characteristics of the structure.

Many constructions show increasing crack development during their service life due to mechanical and environmental loadings. The damage can be translated into a modification of structures mass, damping and stiffness properties. A vast amount of methods exists that examine changes in measured vibration response to detect, locate, and characterize damage in structural and mechanical systems. The basic idea behind these methods is that modal parameters (notably frequencies, mode shapes, and modal damping factors) are functions of the physical properties of the structure (mass, damping, and stiffness). Therefore, changes in the physical properties will cause detectable changes in the modal properties. Literature overview of damage Identification methods using vibration analysis is given, among others, by Doebling, et al. [2], Farrar, et al. [3], [4], [5], and Rytter [6].

Detection methods using changes in modal parameters to identify damage can be subdivided into two distinct approaches. The first approach, which is called “the response-based approach”,

compares modal parameters of the undamaged structure with the modal parameters obtained on the same structure in a damaged condition. The presence and severity of the damage can be assessed by evaluating the changes in natural frequencies and damping ratios. A detailed example of the application of response-based damage detection, by investigating the changes in modal curvatures of a highway bridge can be found in [7].

The second approach, “the model-based approach”, aims at finding a set of model parameters of a mathematical model, in most cases a FE-model, of the considered structure, in order to have an optimal correlation between the experimentally measured and numerically calculated modal parameters. Damage can then be assessed by investigating the obtained model parameters. An application of the model-based concept can be found in [8], where this approach was used to investigate a damaged reinforced concrete beam under laboratory conditions. A general review of the model-based approach can be found in [9].

The response-based approach is a very time efficient way of identifying damage, but these methods have one major drawback, the modal parameters of the undamaged structure have to be known. While the model-based approach demands considerably larger calculation times than the response based approach, it has the major advantage of only needing the modal parameters of the damaged structure. This important quality of the model-based approach opens the way to new application fields of these methods. The elastic material properties of test beam or plates can be identified from vibration behavior as described in [10]. A major assumption made in [10] is the homogeneity of the test samples. This homogeneity assumption is acceptable, without prior verification, in the case of metal test specimen, but in the case of composite materials a preliminary check of the homogeneity would be appropriate. Model-based damage identification could be used as a tool for such an evaluation.

This paper discusses the application of a model-based approach to identify the homogeneity of an undamaged cement beam, and the damage pattern of the same beam after damaging. The results obtained with FEM-updating routine are validated by means of an analytical method called the “Single Point Identification” or “Direct Stiffness Calculation” [11]. The results of both methods confirmed each other.

## 2 The FEM-updating identification routine

Structural damage is typically related to changes in the modal parameters of a structure, and by running a series of FE simulations of a cantilever and a simply supported beam, Pandey *et al.* [12] showed that the modal curvatures are highly sensitive to damage, and that they can be used for damage identification or localization. The modal curvatures are however only sensitive to variations of the longitudinal Young’s modulus of a beam specimen, and can therefore only provide an unscaled stiffness profile. In order to obtain a correct absolute scaling of the stiffness’, resonance frequencies have to be incorporated into the identification procedure.

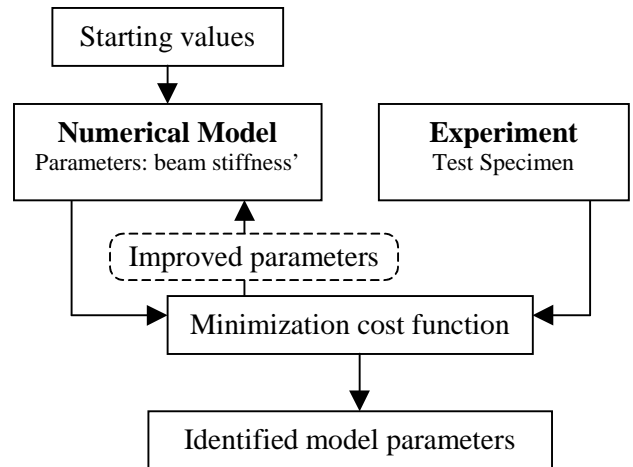


Figure 1: General flowchart of a FEM-updating.

A key step in model-based damage identification is the updating of the finite element model of the structure in such a way that the measured responses can be reproduced by the FE-model. A general flowchart of this operation is given in figure 1. For a complete review of model-updating techniques, the reader is referred to [13]. The identification procedure presented in this paper is a sensitivity based model updating routine. Sensitivity coefficients are the derivatives of the system responses with respect to the model parameters, and are needed in the cost function of the flowchart of figure 1. To improve the conditioning of the optimization problem relative normalized sensitivities [14] can be used (1):

$$s = \frac{\partial R}{\partial P} \frac{P}{R} \quad (1)$$

By using the relative normalized sensitivities the updating procedure will minimize the relative differences instead of the absolute differences between the experimental and calculated responses. The presented updating procedure will identify the longitudinal Young's modulus from the modal curvatures and the resonance frequency of the first vibration mode of a beam. If  $n$  modal curvatures are used to update the Young's moduli of a beam divided into  $k$  zones with uniform material properties, then the sensitivity coefficients can be assembled into a  $(n+1) \times k$  sensitivity matrix:

$$[S]_{(n+1) \times k} = \begin{bmatrix} \frac{\partial w_1^*}{\partial E_1} \frac{E_1}{w_1} & \frac{\partial w_1^*}{\partial E_2} \frac{E_2}{w_1} & \dots & \frac{\partial w_1^*}{\partial E_k} \frac{E_k}{w_1} \\ \vdots & \vdots & \ddots & \vdots \\ \frac{\partial w_n^*}{\partial E_1} \frac{E_1}{w_n} & \frac{\partial w_n^*}{\partial E_2} \frac{E_2}{w_n} & \dots & \frac{\partial w_n^*}{\partial E_k} \frac{E_k}{w_n} \\ \frac{\partial f_1}{\partial E_1} \frac{E_1}{f_1} & \frac{\partial f_1}{\partial E_2} \frac{E_2}{f_1} & \dots & \frac{\partial f_1}{\partial E_k} \frac{E_k}{f_1} \end{bmatrix} \quad (2)$$

Improved model parameters can be found by solving the following least-squares problem

$$\{\Delta P\}_{jk} = [S]_{k \times (n+1)}^T \{\Delta R\}_{n+1} \quad (3)$$

with

$$\Delta P = \frac{P_{new} - P_{old}}{P_{old}} \quad \text{and} \quad \Delta R = \frac{R_{exp} - R_{FE}}{R_{exp}} \quad (4)$$

The use of this pure least squares cost function resulted in a unstable updating procedure, caused by very large changes of the model parameters, changes that partially compensated each other. To eliminate these very large parameter changes, limits on the relative changes of the model parameters had to be imposed. The least-squares problem was rewritten as an optimization problem, and parameter limits were imposed by adding logarithmic barrier functions to the objective function. Finally the optimization problem (5) is obtained:

$$\min_{\{\Delta P\}} \left( \{\Delta P\}^T [S]^T [S] \{\Delta P\} - 2\{\Delta P\}^T [S] + \{\Delta P\}^T \{\Delta P\} + \sum_{i=1}^k \phi_i^{Upper} + \sum_{i=1}^k \phi_i^{Lower} \right) \quad (5)$$

in which

$$\phi_i^{Upper}(\Delta P_i) = \begin{cases} -\log(\alpha_i - \Delta P_i) & \text{if } \Delta P_i < \alpha_i \\ +\infty & \text{if } \Delta P_i \geq \alpha_i \end{cases} \quad (6)$$

$$\phi_i^{Lower}(\Delta P_i) = \begin{cases} -\log(\Delta P_i - \beta_i) & \text{if } \Delta P_i > \beta_i \\ +\infty & \text{if } \Delta P_i \leq \beta_i \end{cases} \quad (7)$$

$\phi_i^{Upper}$  is the barrier function ensuring that  $\Delta P_i$  remains smaller than the limit value  $\alpha_i$ ,  $\phi_i^{Lower}$  implies the lower boundaries  $\beta_i$  on the relative parameter

changes. A detailed description of the use of logarithmic barrier functions for optimization purposes is given in [15].

### 3 Sensitivity analysis

Before the objective function (5) can be evaluated, the elements of the sensitivity matrix (2) have to be calculated. The absolute sensitivity coefficient of the frequencies and modal displacements can be obtained with the formulas of Fox and Kapoor [16]. When only variation of stiffness parameter are taken into account, and mass normalized mode shapes are being used, these formulas are reduced to (8) for the frequency sensitivities and to (9) for the mode shape sensitivities.

$$\frac{\partial f_i}{\partial P_j} = \frac{\{\psi_i\}^T \frac{\partial [K]}{\partial P_j} \{\psi_i\}}{8\pi^2 f_i} \quad (8)$$

$$\frac{\partial \{\psi_i\}}{\partial P_j} = \sum_{r=1, r \neq i}^N \frac{\{\psi_r\}}{4\pi^2 (f_i^2 - f_r^2)} \{\psi_r\}^T \frac{\partial [K]}{\partial P_j} \{\psi_i\} \quad (9)$$

However, not the sensitivity coefficients of the modal displacements but the sensitivity coefficients of the modal curvatures are needed in (5). The absolute sensitivity coefficients of the modal curvatures can be approximated by a first order Taylor expansion in the vicinity of the working point:

$$s_{w_i^*, P_j} = \frac{\partial w_i^*}{\partial P_j} \cong \frac{w_i^*(P_j + \Delta P_j) - w_i^*(P_j)}{\Delta P_j} \quad (10)$$

The easiest way to compute modal curvatures from modal displacements makes use of the central difference approximation [7], i.e.,

$$w_i^* = \frac{(w_{i-1} - 2w_i + w_{i+1}))}{h^2} \quad (11)$$

where  $h$  is the distance between two successive measured locations.

By expressing the modal curvatures in (10) as function of the modal displacements (11), and by regrouping the appropriate terms, the modal curvature sensitivities can be expressed as a function of the sensitivities of the modal displacements (12):

$$s_{w_i^*} = \frac{s_{w_{i+1}} - 2s_{w_i} + s_{w_{i-1}}}{h^2} \quad (12)$$

where the modal displacement sensitivities  $s_{w_i}$  can be calculated with (9). It should be noted that equation (12) is only valid if written with absolute sensitivity coefficients.

## 4 Single Point Identification

To check the results obtained with the FEM-updating routine described in the previous paragraph, the following analytical ‘‘Single Point Identification’’ routine was used.

The dynamic deformation of a vibrating beam with free-free boundary conditions equals the static deflection of the same beam loaded with the distributed pressure  $p(x)$  if

$$p(x) = \rho A \omega^2 w(x) \quad (13)$$

in which  $\rho$  is the mass density of the beam,  $A$  the cross-sectional surface of the beam,  $\omega$  the circular frequency and  $w$  the modal displacements of the considered mode of vibration. Theory of elasticity provides the following relation between the bending moment  $M(x)$  and static deflection  $w$ .

$$EI \frac{d^2 w(x)}{dx^2} = M(x) \quad (14)$$

where  $E$  is the Young’s modulus of the beam and  $I$  is the moment of inertia of the beam’s cross section. The bending moment  $M(x)$  of (14) can be found by integration of the transverse shear force  $Q(x)$ , which can be found by integration of the distributed pressure  $p(x)$  as denoted by the equations of (15).

$$M(x) = \int_0^x Q(\zeta) d\zeta \quad (15)$$

$$Q(x) = \int_0^x p(\zeta) d\zeta$$

Once the bending moment  $M(x)$  is derived, the Young’s modulus of the beam can be evaluated point by point by means of equation (14).

## 5 Results

### 5.1 Identification routine

The FE-model that was used in the FEM updating routine was a one dimensional beam model with free-free boundary conditions and consisted of

51 equally spaced nodes . The beam was divided into 25 subdomains in which the material properties were assumed uniform. A graphical representation of the used model is given in figure 2.

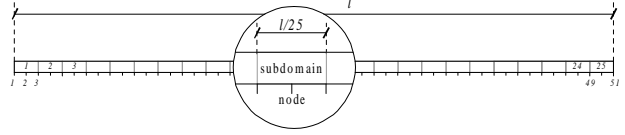


Figure 2: Schematic representation of the used FE-model.

The use of this model gives a  $50 \times 25$  sensitivity matrix, and results in a discrete stiffness profile containing the Young’s moduli of the 25 subdomains of the beam. Values of  $\alpha = 0.5$  and  $\beta = -0.5$  were used for the coefficients barrier function of the constrained minimization problem, which resulted in a fast and smooth convergence of the model parameters. The method was implemented in the commercially available FEMtools software [17] by means of the FBScripting language.

### 5.2 Numerically simulated experiments

In a first step, the proposed procedure was evaluated on numerically generated data of the first vibration modes of two beams with free-free boundary conditions. The resonance frequency and mode shapes of the beams were calculated with the ANSYS FE-software package. The first beam had a constant longitudinal stiffness of 70 GPa, the second beam had a linearly varying longitudinal stiffness profile with a minimum of 45 GPa in the center, a maximal value of 70 GPa at both ends of the beam. Figure 3 shows the starting values and obtained stiffness’ for the uniform beam.

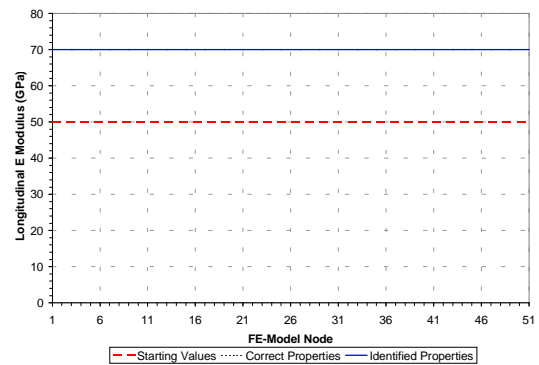


Figure 3: Results obtained on the uniform beam.

Figure 4 shows the initial and obtained stiffness profile of the beam with a linearly varying stiffness

profile, and compares it with the correct longitudinal stiffness distribution.

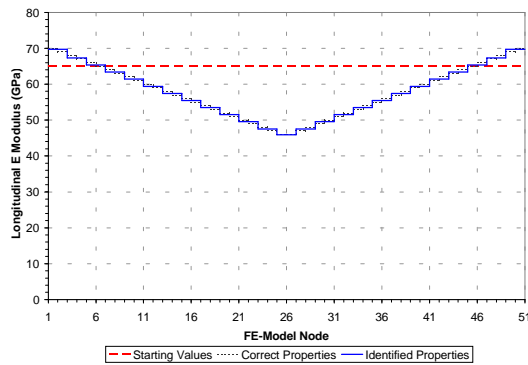


Figure 4: Results obtained on the beam with linearly varying stiffness distribution.

Figure 5 gives the values of the Young's modulus of the 13<sup>th</sup> subdomain – the center of the beam – for the different iteration steps in the case of the beam with the linearly varying stiffness. It can be seen that the procedure has reached convergence after about 5 iterations.

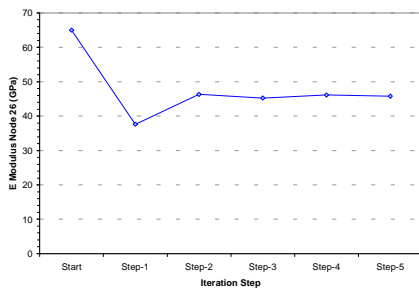


Figure 5: Convergence of the Young's modulus of the 13<sup>th</sup> subdomain, the FE-beam with linearly varying stiffness.

Both examples showed that the FEM-updating routine is able to find the correct longitudinal stiffness distribution from the resonance frequency and modal curvatures of the first mode of a vibrating beam with free-free boundary conditions and this in a stable way.

## 5.3 Experimental results

### 5.3.1 Description of the experiments

In the second stage the presented FEM-model updating method was tested on experimental data, measured on a vibrating glass fiber reinforced IPC beam. IPC: Inorganic Phosphate Cement [18] is a two-component system of a calcium silicate powder

and a phosphate acid based solution of metal oxides. After hardening the IPC's material properties are similar to those of traditional cement materials. One of the major benefits of IPC compared to other cementitious materials is the non-alkaline environment of IPC before and after hardening. Ordinary E-glass fibers are not attacked by the matrix and can thus be used as reinforcement. IPC was used in the present research because this brittle material can be easily damaged.

The IPC beam, with nominal dimensions of  $213 \times 19.5 \times 5$  mm, was suspended to very thin wires attached to the beams on the nodal lines of the first vibration mode. The resonance frequencies and mode shapes were obtained by means of an output only experimental modal analysis. The beam was acoustically excited with a small loudspeaker and a Polytec Scanning Laser Doppler Vibrometer was used to measure the response of the beam to the excitation signal. The scanning area was divided into a regular grid of 3 rows and 213 columns. The 639 measurement points that were hence obtained yielded a spatial resolution of 1 mm in the axial direction of the test beam. The LMS CADA-X v. 3.5C software was used to extract the modal parameters from the measurement data.

After testing and extracting the modal parameters, the IPC beam was damaged. Figure 6 depicts the 3-point bending setup used to induce a controllable amount of damage in the beam. A maximal force  $P$  of 120 N was applied to the center of the beam. During damaging the IPC beam was supported in the vicinity of the modal lines of the first vibration mode. After damaging the modal parameter of the beam were extracted once again.

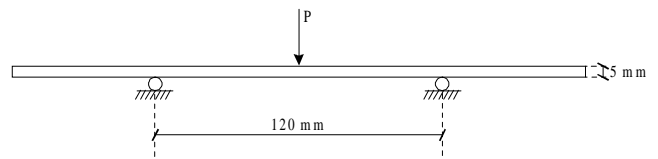


Figure 6: The 3-point bending setup to induce a controllable amount of damage in the IPC beam.

### 5.3.2 Conditioning of the experimental data

Experimental modal displacement data is corrupted with noise, and the influence of the noise becomes worse when the mode shape derivatives are computed. Therefore, the modal curvatures computed from the raw experimental mode shape

were useless. In order to obtain useful modal curvatures, the experimental mode shape was curve fitted by means of a 10<sup>th</sup> order Lagrange polynomial. During the curve fit, the rigid body movements were also eliminated by putting the shear force and bending moment at the end of the beam to zero. A more detailed description of the used smoothing technique is given in [19]. Figure 7 shows the raw and curve fitted mode shape in the center of the undamaged IPC beam, it is obvious that a direct application of equation (11) on the raw mode shape data will result in very noise corrupted modal curvatures.

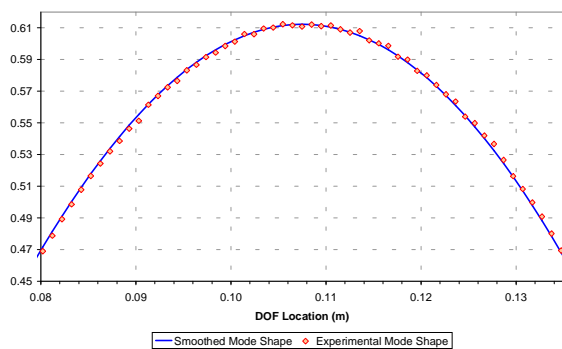


Figure 7: The raw and curve fitted mode shape of the first mode of the undamaged beam.

From this smoothed mode shape, the modal curvatures were derived with equation (11), and the resulting modal curvature curve was sampled at the points that correspond with the modal curvatures obtained from the FE-model of the updating procedure. The sampled modal curvatures of the undamaged and damaged beam are plotted respectively in figure 8 and figure 9.

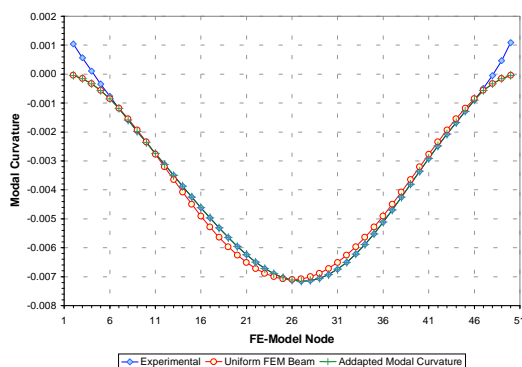


Figure 8: The sampled modal curvatures of the undamaged IPC beam.

Both for the undamaged and damaged beam, positive modal curvatures are found on the both end of the beams. This is physically impossible for

straight beam samples and is caused by a the smoothing of the modal displacement data. The use of these positive modal curvatures had a very negative effect on the stability of the FEM updating procedure. Therefore, the modal curvatures of the ends of the beams were replaced by the theoretically predicted modal curvatures of a uniform beam. On the left side of the beams, five modal curvatures were adapted, on the right side only three curvatures had to be changed. Finally the curves denoted as “Adapted Modal Curvatures” on figures 8 and 9 were obtained, and used in the FEM-updating routine.

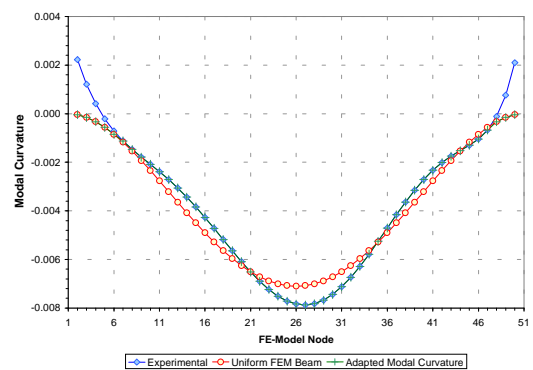


Figure 9: The sampled modal curvatures of the damaged IPC beam.

### 5.3.3 The experimental results

The graph of figure 10 compares the modal curvatures of the FE-model after updating with the experimental curvatures. A good correspondence between experimental and numerical results was obtained, for both the undamaged and damaged IPC beam. Of course, the modal curvature at the end of the beam does not correspond with the experimental modal curvatures, because the positive experimental modal curvatures were replaced by the FEM curvatures of the uniform beam.

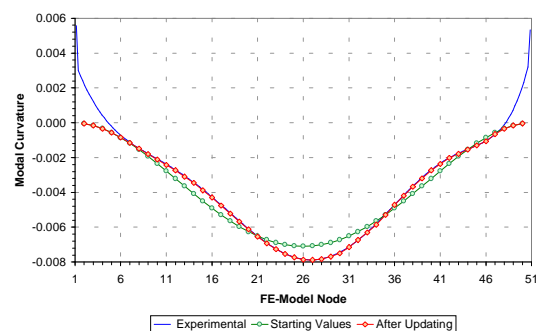


Figure 10: Comparison between the experimental and FE modal curvatures after updating.

Figure 11 gives the longitudinal stiffness distributions obtained with the FEM updating routine for IPC beam in both undamaged and damaged condition. It can be seen that there is a small difference in stiffness between the left and right side of the undamaged beam, in the zone between the nodal lines of the first vibration mode. After damaging, a clear decrease of the stiffness is noticed in the zone between the nodal lines. The identification routine also indicates a decrease in stiffness at the ends of the beams, and a small increase of stiffness at the nodal line position on the right side of the beam. These two phenomena can be explained by comparing the results of the FEM updating routine with the results of the single point identification method.

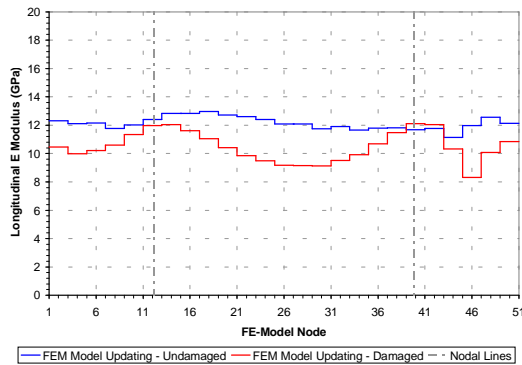


Figure 11: The longitudinal stiffness distribution of the damaged and undamaged beam, as obtained with the FEM updating routine.

Figures 12 and 13 compare the results obtained with the FEM updating routine and the single point identification method. A good agreement between the results of two methods is found in the domain between the nodal lines.

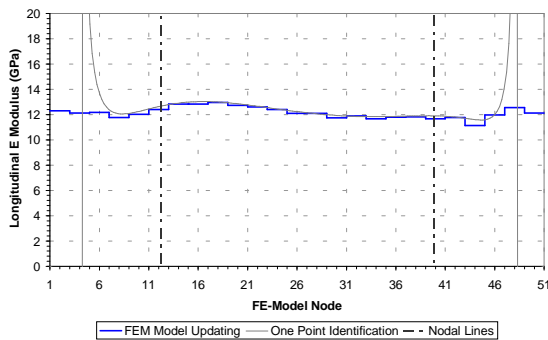


Figure 12: Comparison between the results obtained with the FEM-updating routine and the single point identification of the undamaged beam.

The increase of stiffness for the damaged beam at the position of the right nodal line is also found by the single point identification method, together with the decrease of stiffness in the undamaged zone at the ends of the beams in the vicinity of the nodal lines. This indicates that both the increase at the right nodal line, and the decrease of the stiffness at the beam's ends are caused by the curve fitting algorithm used to smoothen the experimental modal displacements, and are not inherent to the FEM-updating routine.

The negative Young's moduli obtained at the ends of the beams are a result of the positive values of the modal curvatures of the curve fitted experiment data. Since these values were replaced by the theoretical modal curvatures of a homogeneous beam in the FEM-updating routine, the negative E moduli are not found by the updating procedure.

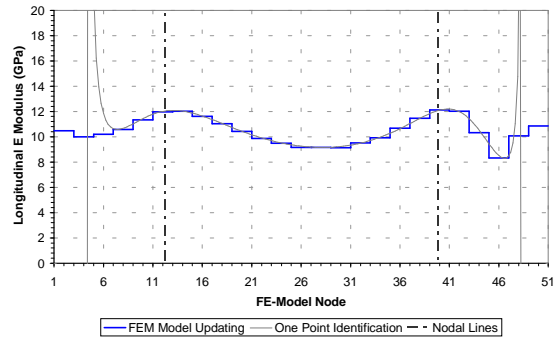


Figure 13: Comparison between the results obtained with the FEM-updating routine and the single point identification of the damaged beam.

## 6 Conclusions

A FEM-updating procedure to identify the longitudinal stiffness profile of a beam specimen from the modal curvatures and resonance frequency of one single vibration mode was presented. The method was evaluated on both numerically generated and experimentally measured data, and proved to behave stable in both cases. The experimental data was obtained on an IPC beam in both undamaged and damaged condition. The application of the FEM-updating procedure resulted in realistic stiffness distribution for both undamaged and damaged beam. The obtained results could be reproduced by means of an analytical single point identification method.



## Acknowledgements

Part of this work was carried out in the framework of the GRAMATIC project, which is financially supported by the Flemish government Institute IWT.

## References

- [1] Doherty, J. E., “*Nondestructive Evaluation*,” Chapter 12 in Handbook on Experimental Mechanics, A. S. Kobayashi Edt., Society for Experimental Mechanics, Inc., 1987.
- [2] Doebling, S. W., Farrar, C. R., Prime, M. B., and Shevitz, D. W. “*Damage Identification and Health Monitoring of Structural and Mechanical Systems from Changes in their Vibration Characteristics: A Literature Review*”, Los Alamos National Laboratory report LA 13070-MS, april 1996
- [3] Farrar, C.R., Doebling, S.W., and Duffey, T.A., “*Vibration-Based Damage Detection*”, presented at the SD2000 Structural Dynamics Forum, April 11-17, 1999.
- [4] Farrar, C.R. and Doebling, S.W., “*An Overview of Modal-Based Damage Identification Methods*”, in Proc. of DAMAS Conference, Sheffield, UK, June 1997.
- [5] Farrar, C.R., Doebling, S.W., Nix, D.A., 2001, “*Vibration-Based Structural Damage Identification*”, Philosophical Transactions of the Royal Society: Mathematical, Physical & Engineering Sciences, Vol. 359, No. 1778, pp. 131 – 149.
- [6] Rytter, A., “*Vibration based inspection of civil engineering structures*,” Ph. D. Dissertation, Department of Building Technology and Structural Engineering, Aalborg University, Denmark, 1993.
- [7] Abdel Wahab, M. M., De Roeck, G., “*Damage detection in bridges using modal curvatures: application to a real damage scenario.*”, Journal of Sound and Vibration, 226(2), 217-235, 1999.
- [8] Abdel Wahab, M. M., De Roeck, G., Peeters, B., “*Parameterization of damage in reinforced concrete structures using model updating*” Journal of Sound and Vibration, 228(4), 717-730, 1999.
- [9] Sol H., “*Identification of Anisotropic Plate Rigidities Using Free Vibration Data*”, PhD. Thesis, Vrije Universiteit Brussel, Belgium, 1986.
- [10] Fritzen, C.-P., Jennewein, D., Kiefer, T., “*Damage detection based on model updating methods*”, Mechanical Systems and Signal Processing, pp. 163-186, 1997.
- [11] Maeck, J., De Roeck, G., “*Damage detection on prestressed concrete bridge and RC beams using dynamic system identification*”, Proceedings DAMAS 99, pages 320–327, Dublin, Ireland, June 1999. Trans Tech Publications Ltd.
- [12] Pandey, A. K., Biswas, M., Sammam, M. M., “*Damage detection from changes in curvature mode shapes*”, Journal of Sound and Vibration 145, 312-332, 1991.
- [13] Friswell, M.E., Mottershead, J.E., “*Finite element updating in structural dynamics*”, Kluwer academic press, 1999.
- [14] “*FEMtools theoretical manual*”, Dynamic Design Solutions NV, Leuven, 2001
- [15] Boyd, S., Vandenberghe, L., “*Convex Optimization with Engineering Applications*”, Course Reader, Stanford University, USA, December 2001.
- [16] Fox, R. L., Kapoor, M. P., “*Rates of changes of eigenvalues and eigenvectors*”, AIAA Journal, Vol. 6., 1968, pp. 2426-2429.
- [17] FEMtools, <http://www.FEMtools.com>, Dynamic Design Solutions NV.
- [18] Wastiels, J., “*Sandwich panels in construction with HPFRCC-faces: New possibilities and adequate modelling*”, Proc. of RILEM, Mainz, Germany, May 16-19, 1999.
- [19] Sol, H., Lauwagie, T., Guillaume, P. “*Identification of distributed material properties using measured modal data*”, Proceeding of the International Seminars on Modal Analysis, 2002, Leuven, Belgium.